Dual roles of an *Arabidopsis* ESCRT component FREE1 in regulating vacuolar protein transport and autophagic degradation

Caiji Gao[a,1], Xiaohong Zhuang[a,1], Yong Cui[a], Xi Fu[a], Yilin He[a], Qiong Zhao[a], Yonglun Zeng[a], Jinbo Shen[a], Ming Luo[a,b], and Liwen Jiang[a,c,2]

[a]Centre for Cell and Developmental Biology and State Key Laboratory of Agrobiotechnology, School of Life Sciences, The Chinese University of Hong Kong, Shatin, New Territories, Hong Kong, China; [b]South China Botanical Garden, Chinese Academy of Sciences, Guangzhou 510650, China; and [c]CUHK Shenzhen Research Institute, The Chinese University of Hong Kong, Shenzhen 518057, China

Edited by Natasha V. Raikhel, Center for Plant Cell Biology, Riverside, CA, and approved January 1, 2015 (received for review November 6, 2014)

Protein turnover can be achieved via the lysosome/vacuole and the autophagic degradation pathways. Evidence has accumulated revealing that efficient autophagic degradation requires functional endosomal sorting complex required for transport (ESCRT) machinery. However, the interplay between the ESCRT machinery and the autophagy regulator remains unclear. Here, we show that FYVE domain protein required for endosomal sorting 1 (FREE1), a recently identified plant-specific ESCRT component essential for multivesicular body (MVB) biogenesis and plant growth, plays roles both in vacuolar protein transport and autophagic degradation. FREE1 also regulates vacuole biogenesis in both seeds and vegetative cells of *Arabidopsis*. Additionally, FREE1 interacts directly with a unique plant autophagy regulator SH3 DOMAIN-CONTAINING PROTEIN2 and associates with the PI3K complex, to regulate the autophagic degradation in plants. Thus, FREE1 plays multiple functional roles in vacuolar protein trafficking and organelle biogenesis as well as in autophagic degradation via a previously unidentified regulatory mechanism of cross-talk between the ESCRT machinery and autophagy process.

FYVE domain | ESCRT machinery | vacuole biogenesis | autophagic degradation | FREE1

The endosomal–lysosomal/vacuolar pathway is the primary catabolic system of eukaryotic cells that degrades extracellular and intracellular materials. Membrane proteins destined for degradation, such as misfolded proteins or endocytosed receptors, become tagged by ubiquitin for further sorting to the endosomal–lysosomal/vacuolar system for degradation (1). During this process, an evolutionarily conserved machinery called endosomal sorting complex required for transport (ESCRT), is responsible for sorting these ubiquitinated cargos into the intraluminal vesicles (ILVs) of prevacuolar compartments/multivesicular bodies (PVCs/MVBs), which subsequently fuse with vacuoles/lysosomes to deliver their contents into the lumen for proteolytic degradation (2, 3). Malfunction of the assembly or dissociation of the ESCRT machinery disrupts MVB formation and thus results in the accumulation of ubiquitinated membrane cargos (4, 5).

Macroautophagy (hereafter as autophagy) is another highly conserved catabolic process, which converges on the endosomal–lysosomal/vacuolar pathway to deliver aberrant organelles, long-lived proteins, and protein aggregates to the lysosome/vacuole via a unique structure termed the "autophagosome" (6). Morphologically different from MVBs, autophagosomes are characterized by a double membrane structure, which is initiated from the phagophore assembly site/preautophagosome site (PAS) (7). The proteins or organelles to be degraded are encapsulated by autophagosomes that fuse either directly with the vacuole/lysosome or with endosomes like MVBs for expansion/maturation to form amphisomes, which then fuse with vacuole/lysosome for degradation. A number of conserved autophagy-related gene (ATG) proteins have been identified as participating in the autophagy pathway in eukaryotic cells (8).

Even though it is generally accepted that at least one population of developing autophagosomes fuses with late endosomal compartments before their fusion with lysosomes, little is known about the functional relationship between the autophagy and endocytic pathways. New light has been thrown onto this situation through the discovery that ESCRT is also involved in autophagy. More and more studies on nematodes, flies, mammals, and even on plants provide evidence to support the conclusion that the inactivation of ESCRT machinery causes an accumulation of autophagosomes (9–13). Different models, such as the induction of autophagy or the disruption of autophagosome–endosome/lysosome fusion, have been proposed to explain the observation that autophagosomes accumulate in ESCRT-depleted cells (14, 15). However, there are no studies to give a direct link between ESCRT machinery and autophagy regulators.

Here, we show that FYVE domain protein required for endosomal sorting 1 (FREE1), which represents a recently identified and unique plant ESCRT component essential for MVB biogenesis (5), plays a crucial role in vacuolar protein transport and vacuole biogenesis. In addition, FREE1 directly interacts with SH3 DOMAIN-CONTAINING PROTEIN2 (SH3P2), a unique regulator in plant autophagy (16), to manipulate the autophagosome–vacuole fusion

Significance

Macroautophagy (hereafter as autophagy) involves the delivery of cytosolic materials via autophagosome upon its fusion with the endosome and lysosome/vacuole. The endosomal sorting complex required for transport (ESCRT) machinery is responsible for the formation of intraluminal vesicles (ILVs) in multivesicular bodies (MVBs) and the sorting of ubiquitinated membrane cargos into MVB ILVs for degradation. Here, we show that, in addition to regulating MVB biogenesis, the plant-specific ESCRT component FYVE domain protein required for endosomal sorting 1 (FREE1) also plays dual roles in vacuolar protein transport and autophagic degradation. FREE1 directly interacts with a plant autophagy regulator SH3 DOMAIN-CONTAINING PROTEIN2 to manipulate the autophagic degradation in plants. Thus, we demonstrate multiple functions of FREE1 and a direct link between the ESCRT machinery and autophagy process in plants.

Author contributions: C.G., X.Z., and L.J. designed research; C.G., X.Z., Y.C., X.F., Y.H., Q.Z., Y.Z., J.S., and M.L. performed research; C.G., X.Z., and L.J. analyzed data; and C.G., X.Z., and L.J. wrote the paper.

The authors declare no conflict of interest.

This article is a PNAS Direct Submission.

[1]C.G. and X.Z. contributed equally to this work.

[2]To whom correspondence should be addressed. Email: ljiang@cuhk.edu.hk.

This article contains supporting information online at www.pnas.org/lookup/suppl/doi:10.1073/pnas.1421271112/-/DCSupplemental.

and finally autophagic degradation in plants. Our studies have thus unveiled a previously unidentified regulatory mechanism for direct cross-talk between the ESCRT machinery and autophagy process.

Results and Discussion

FREE1 Is Required for the Biogenesis of and Protein Transport to Protein Storage Vacuoles. We recently identified a plant-specific FYVE domain protein called FREE1, which functions as an ESCRT component to control the formation of ILVs in PVCs/MVBs (5). In addition, a recent study also demonstrated the function of FREE1/FYVE1 in regulating the polarization of iron-regulated transporter 1 (IRT1) to the plant–soil interface, and the IRT1-dependent metal homeostasis in plant (17). FREE1 is essential for plant growth and FREE1 depletion causes seedling lethality (Fig. S1) (5). To further investigate the possible roles of FREE1 in regulating PVC-mediated vacuolar protein transport and vacuole biogenesis, we crossed the *free1*$^{+/-}$ mutant with a plant expressing the protein storage vacuole (PSV) marker GFP-CT24, which consists of a signal peptide and GFP followed by the C-terminal 24 amino acids of the α′ subunit of β-conglycinin under the control of a seed-specific promoter that is sufficient for sorting to PSVs in *Arabidopsis* seeds (18, 19). Interestingly, large numbers of green seeds under UV light were found in the progenies derived from the self-pollinated *free1*$^{+/-}$ mutant plants expressing GFP-CT24 (Fig. 1*A*). On the contrary, the seeds of WT/GFP-CT24, in which GFP was accumulated in PSVs, only displayed extremely low background signals of GFP fluorescence (Fig. 1*A*). Genotyping confirmed these green seeds to be homozygous *free1* mutants and thus indicated the impairment of protein transport to the PSV in the *free1* mutant. As expected, in the wild-type seeds, GFP-CT24 was predominantly localized in PSVs recognized by their autofluorescence, whereas in the green seeds of *free1* mutants, GFP-CT24 was mostly secreted into the extracellular spaces (Fig. 1*B*). To further verify the PSV transport defect in the *free1* mutant, the homozygous *free1* seeds identified by their green signals due to secretion of the GFP-CT24 marker were collected for storage protein profile analysis. As shown in Fig. 1*C*, the *free1* mutant showed strong defects in storage protein processing and accumulated precursors of storage proteins as indicated by Coomassie blue staining and immunoblots with 12S globulin and 2S albumin antibodies. In addition to the mistargeting of storage proteins, the PSVs in the *free1* mutant were much smaller than in WT seeds, suggesting a role of FREE1 for PSV biogenesis (Fig. S2).

To further examine the role of FREE1 in protein transport to PSVs, we next analyzed the vacuolar trafficking of newly synthesized proteases and the mobilization of storage proteins in seeds of *dexamethasone* (*DEX*)*-inducible RNAi-FREE1* plants after germination in the presence or absence of DEX. During seed germination proteases, such as aleurain, will be synthesized in the endoplasmic reticulum (ER) and transported to vacuoles where they attain a mature form, allowing them to degrade the storage proteins to provide energy for seed germination and amino acids for early stages of seedling growth (19, 20). Here, we detected a strong accumulation of the precursor form of aleurain in *DEX::RNAi-FREE1* seedlings germinated in the presence of DEX (Fig. S3*A*). Correspondingly, degradation of the storage proteins, 12S globulin and 2S albumin, was significantly delayed in *DEX::RNAi-FREE1* seedlings under the DEX-induced condition (Fig. S3*A*). Similarly, delayed degradation of storage proteins in *FREE1*-knockdown plants was further supported by using the PSV marker GFP-CT24 in germinating seedlings. Similar to WT, GFP-CT24 accumulated in PSVs in mature *DEX::RNAi-FREE1* seeds at 0 d after germination (DAG) (Fig. S3*B*). In the *DEX::RNAi-FREE1* seedlings at 4 DAG germinated on the plate without DEX, the PSV-localized GFP-CT24 signal was almost completely disappeared due to degradation (Fig. S3 *B* and *C*). However, in the *DEX::RNAi-FREE1* seedlings at 4 DAG on the plate containing DEX, strong GFP-CT24 signal could still be detected in the vacuoles (Fig. S3 *B* and *C*), which could be due to the vacuolar trafficking defect of the proteases such as aleurain caused by the depletion of FREE1. Together, these results showed that FREE1 plays a crucial role in PSV biogenesis and transport of storage vacuolar proteins.

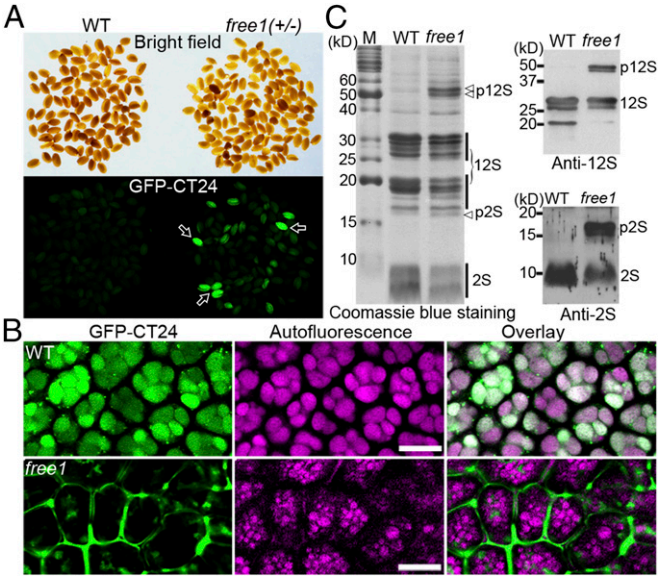

Fig. 1. FREE1 regulates the transport of vacuolar proteins to protein storage vacuoles. (*A*) The *free1* mutant is defective in the transport of seed storage proteins. GFP-CT24 was expressed in the wild-type (WT) and *free1* ($^{+/-}$) heterozygous plants. The seeds of the F2 population were inspected with a fluorescence microscope. *free1*/GFP-CT24 produced green fluorescent seeds (arrows). (*B*) The GFP-CT24 is targeted to protein storage vacuoles in wild-type seed cells, whereas it is secreted to the extracellular spaces in *free1* mutant cells. (Scale bars, 10 μm.) (*C*) The *free1* mutant is defective in processing of seed storage proteins. The wild-type seeds and the selected green fluorescent seeds shown in *A* were subjected to protein extraction for Coomassie blue staining or immunoblot analysis with GFP and 12S globulin antibodies. Note the accumulation of precursors of storage proteins in *free1* mutant seeds.

Loss of FREE1 Impairs the Formation of and Protein Transport to Lytic Vacuoles. We next examined the fate of protein transport route to lytic vacuoles in *free1* by crossing the *free1*$^{+/-}$ mutant with the lytic vacuolar cargo spL-RFP, which consists of an RFP fusion with the signal peptide and the sequence-specific vacuolar sorting signal of proricin for targeting to lytic vacuoles (21). Contrary to the wild-type plants, in which the soluble vacuole cargo spL-RFP was exclusively transported to the lumen of central vacuole, in the *free1* mutant this artificial cargo was partially secreted to the extracellular spaces (Fig. 2 *A* and *B*). To gain insight into the fate of the central vacuole in *free1* mutants, we next examined the localization of the vacuolar membrane marker YFP–vesicle-associated membrane protein 711 (VAMP711) (22). In contrast to wild-type plants, in which YFP-VAMP711 labeled the membrane of the large central vacuoles of the cells in cotyledon and root elongation zone (Fig. 2 *C* and *D*), the *free1* mutant lacked large central vacuoles but instead contained numerous fragmented vacuoles marked by YFP-VAMP711 (Fig. 2 *E* and *F*). A further examination of vacuolar protein transport and vacuolar morphology in DEX-treated *DEX::RNAi-FREE1* plant revealed similar results showing the lack of a central vacuole and secretion of soluble vacuolar cargo (Fig. S4). Thus, FREE1 also plays an important role in the formation of large central vacuole in plant cells.

To further gain insight into the effects of the *free1* mutation at the ultrastructural level, we next performed transmission electron microscopic (TEM) analysis of ultrathin sections of *free1*

PLANT BIOLOGY

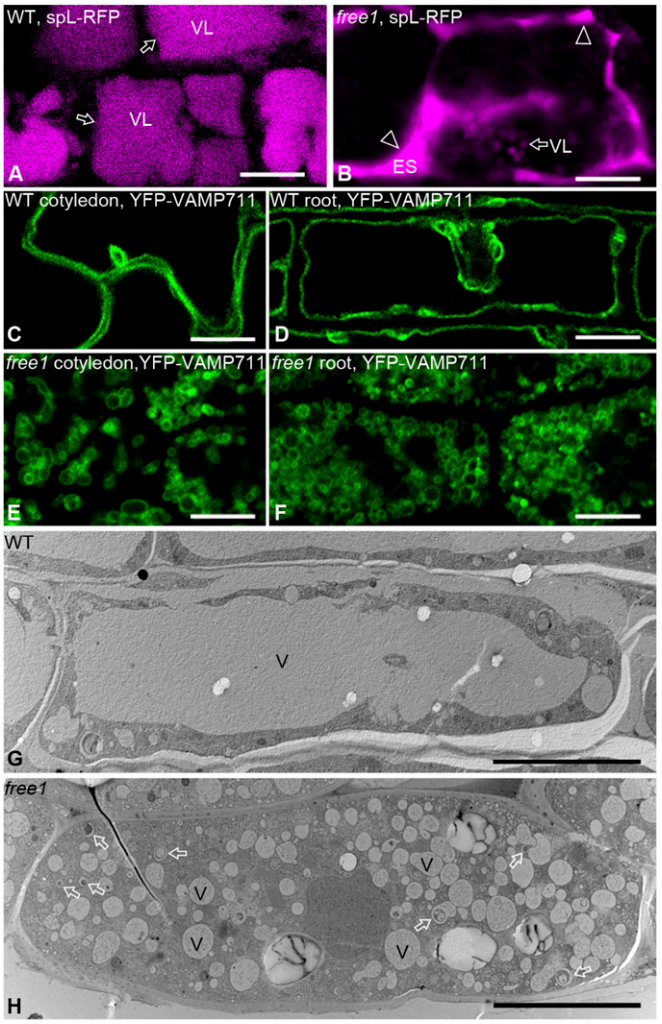

Fig. 2. FREE1 regulates the formation of the central vacuole and the transport of vacuolar proteins to lytic vacuoles. (*A* and *B*) Secretion of vacuolar cargo in *free1* mutant. The soluble vacuolar cargo spL-RFP was localized to the vacuolar lumen (VL) in wild-type plant (arrows) but was largely secreted to the extracellular spaces (ESs) in *free1* mutant (arrowheads). (Scale bars, 10 μm.) (*C–F*) Confocal microscopic images of the vacuolar membrane marker YFP-VAMP711 expressed in the root and cotyledon cells of wild-type and *free1* mutant plants. (Scale bars, 10 μm.) (*G* and *H*) Transmission electron micrographs of root epidermis cells of high-pressure frozen/freeze-substituted wild-type and *free1* mutant seedlings. Note the accumulation of small vacuoles (V) and autophagosomes (arrows) in the *free1* mutant. (Scale bars, 10 μm.)

mutant seedlings processed by high pressure freezing/freeze-substitution (HPF/FS) (23). Consistent with the confocal observation in Fig. 2 *C–F*, the central lytic vacuole, which occupied a large part of the intracellular space in the cells of the elongation zone of the wild-type root tips, was instead changed into numerous small vacuoles in the cells of the *free1* mutant (Fig. 2 *G* and *H*). In addition to the loss of the central lytic vacuole, our TEM analysis also revealed another striking phenomenon: the *free1* mutant accumulates large numbers of autophagosomes identified by their double- or multimembrane structure (Fig. 2*H*).

FREE1 Depletion Causes Accumulation of Autophagosomes. To further examine the accumulation of autophagosomes in the *free1* mutant, we next crossed the *free1*$^{+/-}$ mutant with a plant expressing the fluorescently tagged autophagosome marker enhanced yellow fluorescent protein (EYFP)–autophagy-related gene 8e (ATG8e) (16). In contrast to wild-type plants in which EYFP-ATG8e mainly showed cytosolic localizations with only few punctae indicating the occurrence of a basal level of autophagy, the *free1* mutant accumulated large amounts of EYFP-ATG8e punctate compartments (Fig. 3*A*). A close examination of ultrathin sections of *free1*/YFP-ATG8e root tips by immunogold EM with GFP antibodies also confirmed the accumulations of autophagosomes and the labeling of EYFP-ATG8e to autophagosomes in the *free1* mutant (Fig. 3 *B* and *C* and Fig. S5). Further support for the accumulation of autophagosomes in the *free1* mutants came from the observation that the mutants have strong increased levels of lipidated ATG8, a phosphatidylethanolamine (PE)-conjugated form of ATG8 (ATG8-PE), which labels the forming/completed autophagosomes and is partially degraded upon the fusion of autophagosomes with lysosomes/vacuoles (Fig. 3*D*) (24). Together with the above results showing the involvement of FREE1 in vacuolar protein transport and vacuole formation, the accumulation of autophagsomes and the strong increase of ATG8-PE but not free ATG8 points to defects in membrane fusions between endosomes or autophagosomes and vacuoles but not the induction of autophagy due to FREE1 depletion (25).

FREE1 Interacts with the Autophagosomal Regulator SH3P2 to Mediate the Interplay Between ESCRT and Autophagy Pathways. Several reports in fly and mammalian cells have revealed that an inactivation of the ESCRT machinery causes the accumulation of autophagosomes and one of the most plausible reasons might be due to the blockage of the fusion of autophagosomes with the endolysosomal system (9–11, 15, 26). However, a direct molecular link between ESCRT and autophagy machineries is still lacking. To explore the possible molecular mechanisms of FREE1 function in autophagy, we next cloned several plant

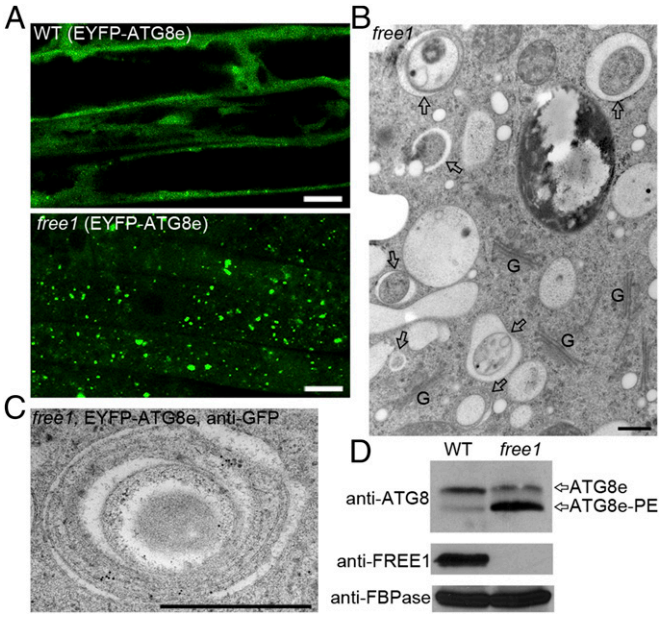

Fig. 3. FREE1 depletion causes the accumulation of autophagosomes. (*A*) Confocal microscopic images of the autophagosome marker EYFP-ATG8e expressed in the roots of wild-type and *free1* mutant plants. (Scale bars, 10 μm.) (*B*) TEM image of *free1* mutant root cells after high-pressure freezing/freeze substitution. Arrows indicate the autophagosomes. G, Golgi apparatus. (Scale bar, 500 nm.) (*C*) Immunogold labeling with GFP antibody in the ultrathin sections of high-pressure freezing/freeze substitution prepared *free1*/EYFP-ATG8e root. (Scale bar, 500 nm.) (*D*) Immunoblots of total protein extracts from wild-type and *free1* seedlings using ATG8e, FREE1, and FBPase (loading control) antibodies.

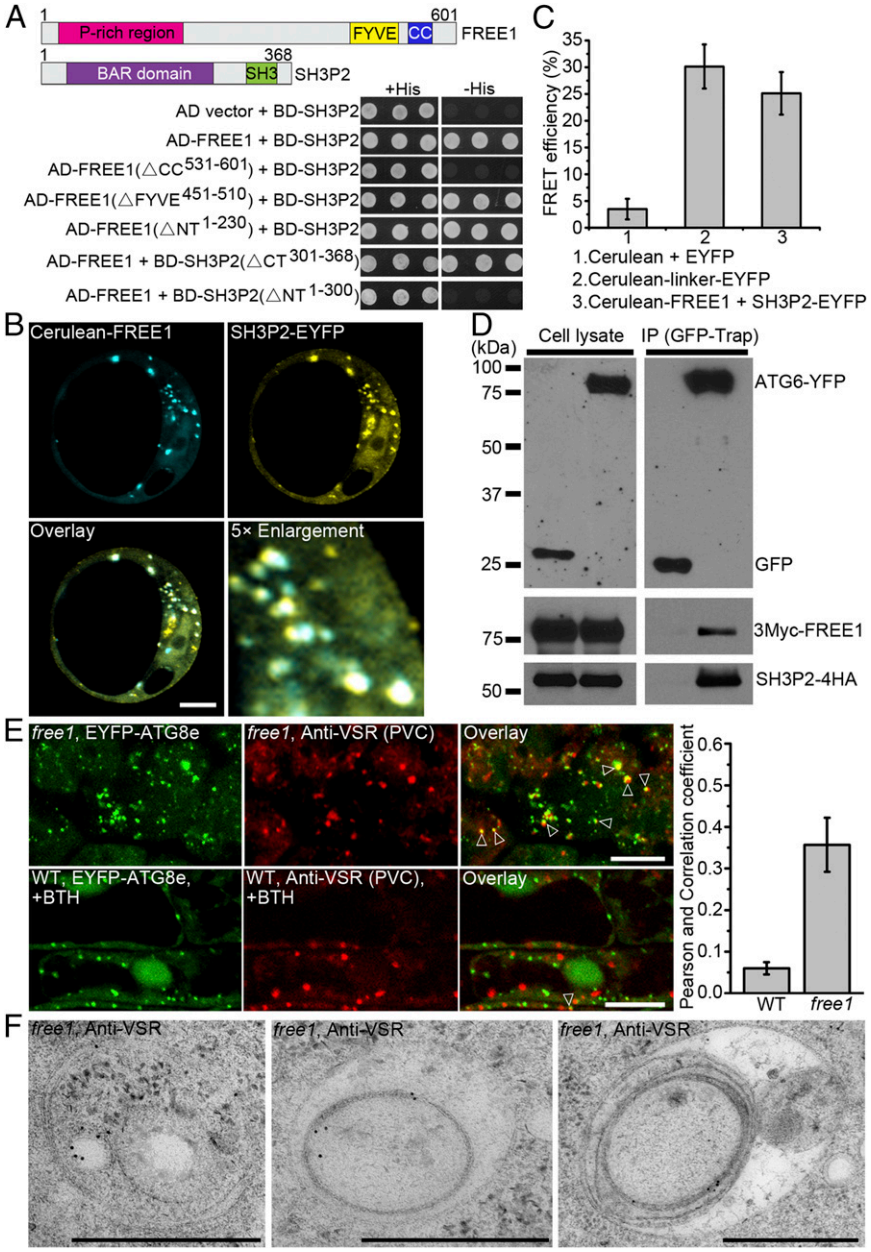

Fig. 4. FREE1 directly interacts with the autophagy regulator, SH3P2, and affects the association between autophagosomes and MVBs. (*A*) Y2H analysis of the binary interactions between SH3P2 with FREE1 or their deletion mutants. (*B*) Partial colocalizations of Cerulean-FREE1 and SH3P2-EYFP expressed in *Arabidopsis* protoplasts. (Scale bar, 10 μm.) (*C*) FRET analysis of the colocalized punctae between Cerulean-FREE1 and SH3P2-EYFP as shown in *B*. FRET efficiency was quantified by using the acceptor photobleaching approach as described in *Materials and Methods*. For each group, at least 10 individual protoplasts were used for FRET efficiency quantification and statistical analysis. (*D*) Immunoprecipitation (IP) assay shows association between FREE1 and SH3P2 with the PI3K complex subunit ATG6. *Arabidopsis* protoplasts expressing GFP or ATG6-YFP with 3Myc-FREE1 and SH3P2-4HA were subjected to protein extraction and IP with GFP-trap followed by immunoblotting with indicated antibodies. (*E*) Immunofluorescent labeling with the PVC marker anti-VSR antibody in BTH-treated wild-type plant expressing the autophagosome marker EYFP-ATG8e or the *free1* mutant expressing EYFP-ATG8e. ImageJ program with the Pearson–Spearman correlation (PSC) colocalization plug-in as described in *SI Materials and Methods* was used to quantify the colocalizations between EYFP-ATG8e and anti-VSR labeling from four individual labeling roots. (Scale bars, 10 μm.) (*F*) Immunogold labeling with anti-VSR antibodies in the ultrathin sections of high-pressure freezing/freeze substitution prepared *free1* mutant root. (Scale bars, 500 nm.)

autophagy regulators for interaction study with FREE1. In the yeast two-hybrid analyses as shown in Fig. 4*A* and Fig. S6, we found that FREE1 did not interact with the ATG8 proteins but showed a clear interaction with SH3P2, which has been shown to associate with the PI3K complex and interact with ATG8 proteins to regulate the formation of autophagosomes (16). When transiently coexpressed in *Arabidopsis* protoplasts, Cerulean-FREE1 and SH3P2-EYFP showed clear punctate dots that substantially colocalized (Fig. 4*B*). The acceptor photobleaching-fluorescence resonance energy transfer (FRET-AB) analysis further confirmed an in vivo interaction between FREE1 and SH3P2 in these colocalized punctae (Fig. 4*C*).

To clarify the domains that mediate the interaction between FREE1 and SH3P2, several mutants harboring domain truncations were used for an interaction analysis of these two proteins. As shown in Fig. 4*A*, the C-terminal coiled-coil region of FREE1

and the N-terminal Bin–amphiphysin–Rvs (BAR) domain part of SH3P2 are essential for the interaction between these two proteins. In addition, both SH3P2 and FREE1 were immunoprecipated by ATG6-YFP, indicating the formation of a PI3K complex by these three proteins (Fig. 4*D*). In combination with our previous report showing that FREE1 specifically interacts with the plant ESCRT-I component vacuolar protein sorting 23 (Vps23) via the PTAP-like tetrapeptide motifs residing in the N-terminal Prorich region (5), these results together support a scenario in which FREE1 might perform at least dual functions: (*i*) regulation of the MVB biogenesis via the incorporation to ESCRT machinery through the N-terminal domain and (*ii*) regulation of autophagy via the link with SH3P2 through the C-terminal domain.

FREE1 Depletion Increases the Association Between Autophagosomes and PVCs/MVBs. In mammalian cells, it has been found that autophagosomes can either fuse directly with lysosomes or fuse first with endosomes to form intermediate compartments called amphisomes, which subsequently fuse with the lysosome (6). In plants, the exact role of MVBs in autophagy remains elusive, even though a recent report has demonstrated a requirement for ESCRT-III in autophagic degradation (13). Because FREE1 is essential for the proper formation of MVBs, it is likely that loss of FREE1 might inhibit either the fusion of autophagosomes with MVBs or the fusion of amphisomes with vacuoles. To address this issue, we next performed immunofluorescence labeling with anti-vacuolar sorting receptor (VSR) antibodies, an MVB marker, in wild-type and *free1* mutant plants expressing the autophagosome marker EYFP-ATG8e. Associations between VSR-labeled MVBs and EYFP-ATG8e–labled autophagosomes were only occasionally detected in wild-type plants treated with benzo-(1,2,3)-thiadiazole-7-carbothioic acid *S*-methyl ester (BTH), a salicylic acid agonist that triggers the autophagic pathway in *Arabidopsis* (27), but were much more frequently observed in the *free1* mutant (Fig. 4*E*). The statistical analysis showed that the colocalization ratio between EYFP-ATG8e and anti-VSR labeling in the *free1* mutant was around five times more than that in BTH-treated wild-type plant (Fig. 4*E*). To further elucidate the autophagosome localization of MVB markers, immunogold EM labeling with VSR antibodies was carried out on ultrathin sections of HPF root tips of the *free1* mutant. Besides the labeling on empty MVBs as shown previously (5), VSR labeling could also be readily found in autophagosomes, especially those with double- or multilayer structures, which might represent the complete fusions of autophagosomes and empty MVBs in the *free1* mutant (Fig. 4*F*).

Autophagic Degradation Is Impeded in the *free1* Mutant. The above results showed that loss of function of FREE1 did not block but rather promoted the fusion between autophagosomes and MVBs. Because the total number of autophagosomes increased greatly in the *free1* mutant, it is likely that loss of FREE1 might inhibit the fusion between autophagosomes or amphisosomes with vacuole. We next tested this hypothesis by treating with Concanamycin A (Conc A), which acts as a V-ATPase inhibitor causing deacidification of the vacuolar lumen and thus the inhibition of degradation of autophagic bodies in the vacuole (16). Consistent with the previous observations of Conc A effect on autophagy, Conc A treatment led to the accumulation of autophagic bodies positive for EYFP-ATG8e in the lumen of the vacuole marked by the vacuolar membrane marker mCherry-VAMP711 in wild-type plant (Fig. 5*A*). Strikingly, the vacuolar accumulation of EYFP-ATG8e–positive autophagic bodies was much less in the *free1* mutant and in DEX-treated *DEX::RNAi-FREE1* plants (Fig. 5 *B* and *C*). These results suggest that the final fusions between autophagosomes or amphisomes with the vacuole are impaired by FREE1 depletion. Alternatively, the decreased vacuolar turnover of autophagosomes in FREE1-depleted cells might also be due to the perturbed vacuolar function, because both vacuolar protein transport and vacuole biogenesis are disrupted in *free1* mutant and in FREE1-RNAi plants.

In summary, we have demonstrated that loss of FREE1 function causes severe defects in vacuolar protein transport, vacuole biogenesis, and the vacuolar degradation of autophagosomes. The facts that FREE1 interacts with either the ESCRT-I subunit Vps23 via the N-terminal PTAP motifs to regulate MVB biogenesis (5), or the autophagy regulator SH3P2 via the C-terminal coiled-coil region to regulate autophagic degradation (this study) demonstrates multiple functions for FREE1 in intracellular trafficking. All of the abnormalities including the dysfunction of vacuolar protein transport and autophagic degradation point to

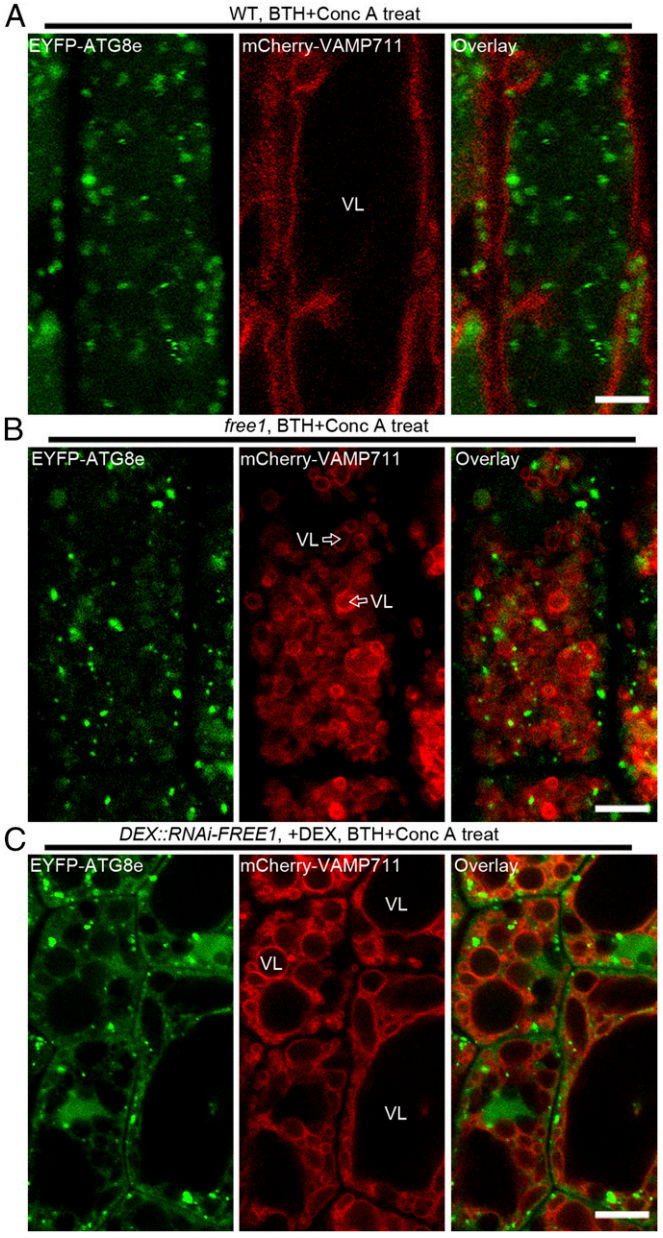

Fig. 5. FREE1 regulates the vacuolar degradation of autophagosomes. The wild-type (*A*), *free1* mutant (*B*), and the DEX-treated *DEX::RNAi-FREE1* (*C*) plants expressing the autophagosome marker EYFP-ATG8e and the vacuolar membrane marker mCherry-VAMP711 were subjected to BTH (100 μM) and Conc A (0.5 μM) treatment for 8 h followed by confocal observation. Note the accumulation of autophagosomes in the vacuolar lumen (VL) in wild-type plant but not in *free1* mutant and *FREE1* RNAi plants. (Scale bars, 10 μm.)

a defect in membrane fusion caused by FREE1 depletion. Until now, a direct function of the ESCRT machinery in the fusion event between vesicles or autophagosomes and lysosomes/vacuoles has remained unknown. It is very likely that the functions of proteins required for docking and/or fusion with vacuoles might be disrupted in the *free1* mutant. Indeed such a hypothesis is supported by the finding that ESCRT proteins can interact with homotypic fusion and vacuole protein sorting (HOPS) complex and less Rab7 GTPase is recruited to the endosomal membrane in the ESCRT mutant (14, 28). In addition, both the HOPS complex and Rab7 have been shown to directly regulate the fusion between autophagosome and vacuole/lysosome (29–32). An interaction between FREE1 and SH3P2 puts the ESCRT machinery into a functional context with the autophagy pathway. Additionally, considering the facts that both FREE1 and SH3P2 bind to PI3P lipid and both of them associate with ATG6 in the PI3K complex, it is possible that FREE1 and SH3P2 might coordinate together to function in a unique plant PI3K complex, to regulate the expansion or maturation of autophagosomes (16). The possible interactions between ESCRT machinery with the HOPS complex might provide the functional basis of FREE1 in manipulating the vacuolar degradation of autophagosomes or amphisomes.

Materials and Methods

Additional materials and methods including plant materials, antibodies, plasmid construction, immunoprecipitation, electron microscopy, confocal microscopy, and yeast two hybrid are described in *SI Materials and Methods*.

Plant Materials. The *Arabidopsis* transposon insertion line of *free1* was obtained from RIKEN. The *DEX-inducible RNAi-FREE1* transgenic plant was generated as described previously (5). Seeds were surface sterilized and grown on plates with half-strength Murashige and Skoog (MS) salts plus 1% sucrose and 0.8% agar at 22 °C under a long-day (16 h light/8 h dark) photoperiod. For induction of *DEX::RNAi-FREE1*, 10 μM DEX (10 mM stock dissolved in ethanol) was added in the medium. Details regarding plant materials, including drug treatment and the procedures for generation and screening of transgenic *Arabidopsis* plant, are described in *SI Materials and Methods*.

Transmission Electron Microscopy. The general procedures for TEM sample preparation, thin sectioning, and immunogold labeling were performed essentially as described previously (16, 23). Root tips of 7-d-old wild-type and *free1* mutant *Arabidopsis* plants were cut and immediately frozen in a high-pressure freezer (EM PACT2, Leica), followed by subsequent freeze substitution in dry acetone containing 0.1% uranyl acetate at −85 °C in an AFS freeze-substitution unit (Leica). Infiltration with HM20, embedding, and UV polymerization were performed stepwise at −35 °C for wild-type plant and −10 °C for the *free1* mutant. Details regarding immunogold labeling and TEM observation are available in *SI Materials and Methods*.

Confocal Microscopy and Acceptor Photobleaching FRET Analysis. The confocal images were captured using the Leica SP8 laser scanning confocal system. The settings for collecting Cerulean, GFP, EYFP, mRFP, and mCherry signals were done according to the manufacturer's instructions. Line sequential scanning mode was always selected in dual-channel observation to avoid the possible cross-talk between two fluorophores. Acceptor photobleaching FRET analysis was conducted on the Leica SP8 confocal system. Briefly, cells expressing various Cerulean and EYFP fusions were used for photobleaching using 514 nm laser in full power intensity. Cerulean donor fluorescence was imaged before and after bleaching a region of interest (ROI) of EYFP to less than 10% of its initial intensity. FRET efficiency was calculated as $Ef = 100 \times (IPost - Ipre)/Ipost$, where Ipre and Ipost stand for the Cerulean intensities before and after acceptor bleaching, respectively.

ACKNOWLEDGMENTS. We thank Prof. Lorenzo Frigerio (University of Warwick) for sharing transgenic plants expressing spL-RFP, Prof. Nobuyuki Maruyama (Kyoto University) for sharing the plasmid encoding GFP-CT24, and Prof. Ikuko Hara-Nishimura (Kyoto University) for providing us the anti-12S and anti-2S antibodies. This work was supported by grants from the Research Grants Council of Hong Kong (CUHK466011, 46112, 466613, CUHK2/CRF/11G, HKUST10/CRF/12R, HKUST12/CRF/13G, and AoE/M-05/12), NSFC/RGC (N_CUHK406/12), the National Natural Science Foundation of China (31270226), the Chinese Academy of Sciences–Croucher Funding Scheme for Joint Laboratories, and Shenzhen Peacock Project (KQTD201101) (to L.J.).

1. Piper RC, Luzio JP (2007) Ubiquitin-dependent sorting of integral membrane proteins for degradation in lysosomes. *Curr Opin Cell Biol* 19(4):459–465.
2. Henne WM, Buchkovich NJ, Emr SD (2011) The ESCRT pathway. *Dev Cell* 21(1):77–91.
3. Winter V, Hauser MT (2006) Exploring the ESCRTing machinery in eukaryotes. *Trends Plant Sci* 11(3):115–123.
4. Shields SB, Piper RC (2011) How ubiquitin functions with ESCRTs. *Traffic* 12(10): 1306–1317.
5. Gao C, et al. (2014) A unique plant ESCRT component, FREE1, regulates multivesicular body protein sorting and plant growth. *Curr Biol* 24(21):2556–2563.
6. Mizushima N, Komatsu M (2011) Autophagy: Renovation of cells and tissues. *Cell* 147(4):728–741.
7. Xie Z, Klionsky DJ (2007) Autophagosome formation: Core machinery and adaptations. *Nat Cell Biol* 9(10):1102–1109.
8. Mizushima N, Yoshimori T, Ohsumi Y (2011) The role of Atg proteins in autophagosome formation. *Annu Rev Cell Dev Biol* 27:107–132.
9. Lee JA, Beigneux A, Ahmad ST, Young SG, Gao FB (2007) ESCRT-III dysfunction causes autophagosome accumulation and neurodegeneration. *Curr Biol* 17(18):1561–1567.
10. Rusten TE, et al. (2007) ESCRTs and Fab1 regulate distinct steps of autophagy. *Curr Biol* 17(20):1817–1825.
11. Filimonenko M, et al. (2007) Functional multivesicular bodies are required for autophagic clearance of protein aggregates associated with neurodegenerative disease. *J Cell Biol* 179(3):485–500.
12. Djeddi A, et al. (2012) Induction of autophagy in ESCRT mutants is an adaptive response for cell survival in C. elegans. *J Cell Sci* 125(Pt 3):685–694.
13. Katsiarimpa A, et al. (2013) The deubiquitinating enzyme AMSH1 and the ESCRT-III subunit VPS2.1 are required for autophagic degradation in Arabidopsis. *Plant Cell* 25(6):2236–2252.
14. Metcalf D, Isaacs AM (2010) The role of ESCRT proteins in fusion events involving lysosomes, endosomes and autophagosomes. *Biochem Soc Trans* 38(6):1469–1473.
15. Rusten TE, Stenmark H (2009) How do ESCRT proteins control autophagy? *J Cell Sci* 122(Pt 13):2179–2183.
16. Zhuang X, et al. (2013) A BAR-domain protein SH3P2, which binds to phosphatidylinositol 3-phosphate and ATG8, regulates autophagosome formation in Arabidopsis. *Plant Cell* 25(11):4596–4615.
17. Barberon M, et al. (2014) Polarization of IRON-REGULATED TRANSPORTER 1 (IRT1) to the plant-soil interface plays crucial role in metal homeostasis. *Proc Natl Acad Sci USA* 111(22):8293–8298.
18. Fuji K, et al. (2007) Arabidopsis vacuolar sorting mutants (green fluorescent seed) can be identified efficiently by secretion of vacuole-targeted green fluorescent protein in their seeds. *Plant Cell* 19(2):597–609.
19. Cui Y, et al. (2014) Activation of the Rab7 GTPase by the MON1-CCZ1 complex is essential for PVC-to-vacuole trafficking and plant growth in Arabidopsis. *Plant Cell* 26(5):2080–2097.
20. Holwerda BC, Padgett HS, Rogers JC (1992) Proaleurain vacuolar targeting is mediated by short contiguous peptide interactions. *Plant Cell* 4(3):307–318.
21. Hunter PR, Craddock CP, Di Benedetto S, Roberts LM, Frigerio L (2007) Fluorescent reporter proteins for the tonoplast and the vacuolar lumen identify a single vacuolar compartment in Arabidopsis cells. *Plant Physiol* 145(4):1371–1382.
22. Geldner N, et al. (2009) Rapid, combinatorial analysis of membrane compartments in intact plants with a multicolor marker set. *Plant J* 59(1):169–178.
23. Gao C, et al. (2012) The Golgi-localized Arabidopsis endomembrane protein12 contains both endoplasmic reticulum export and Golgi retention signals at its C terminus. *Plant Cell* 24(5):2086–2104.
24. Li F, Vierstra RD (2012) Autophagy: A multifaceted intracellular system for bulk and selective recycling. *Trends Plant Sci* 17(9):526–537.
25. Mizushima N, Yoshimori T, Levine B (2010) Methods in mammalian autophagy research. *Cell* 140(3):313–326.
26. Rusten TE, Simonsen A (2008) ESCRT functions in autophagy and associated disease. *Cell Cycle* 7(9):1166–1172.
27. Yoshimoto K, et al. (2009) Autophagy negatively regulates cell death by controlling NPR1-dependent salicylic acid signaling during senescence and the innate immune response in Arabidopsis. *Plant Cell* 21(9):2914–2927.
28. Urwin H, et al.; FReJA Consortium (2010) Disruption of endocytic trafficking in frontotemporal dementia with CHMP2B mutations. *Hum Mol Genet* 19(11): 2228–2238.
29. Jiang P, et al. (2014) The HOPS complex mediates autophagosome-lysosome fusion through interaction with syntaxin 17. *Mol Biol Cell* 25(8):1327–1337.
30. Takáts S, et al. (2014) Interaction of the HOPS complex with Syntaxin 17 mediates autophagosome clearance in Drosophila. *Mol Biol Cell* 25(8):1338–1354.
31. Jäger S, et al. (2004) Role for Rab7 in maturation of late autophagic vacuoles. *J Cell Sci* 117(Pt 20):4837–4848.
32. Liang C, et al. (2008) Beclin1-binding UVRAG targets the class C Vps complex to coordinate autophagosome maturation and endocytic trafficking. *Nat Cell Biol* 10(7): 776–787.